

Bypassing Backdoor Detection Algorithms in Deep Learning

Te Juin Lester Tan

National University of Singapore
lester.tan@comp.nus.edu.sg

Reza Shokri

National University of Singapore
reza@comp.nus.edu.sg

ABSTRACT

Deep learning models are known to be vulnerable to various adversarial manipulations of the training data, model parameters, and input data. In particular, an adversary can modify the training data and model parameters to embed backdoors into the model, so the model behaves according to the adversary’s objective if the input contains the backdoor features (e.g., a stamp on an image). The poisoned model’s behavior on clean data, however, remains unchanged. Many detection algorithms are designed to detect backdoors on input samples or model activation functions, in order to remove the backdoor. These algorithms rely on the statistical difference between the latent representations of backdoor-enabled and clean input data in the poisoned model. In this paper, we design an adversarial backdoor embedding algorithm that can bypass the existing detection algorithms including the state-of-the-art techniques (published in IEEE S&P 2019 and NeurIPS 2018). We design a strategic adversarial training that optimizes the original loss function of the model, and also maximizes the indistinguishability of the hidden representations of poisoned data and clean data. We show the effectiveness of our attack on multiple datasets and model architectures. This work calls for designing adversary-aware defense mechanisms for backdoor detection algorithms.

KEYWORDS

Adversarial Machine Learning, Deep Learning, Backdoors

1 INTRODUCTION

Deep learning models with a large set of parameters and a huge learning capacity can learn very complex tasks with a high predictive power. They are, however, vulnerable to many privacy (which are mostly passive) and security (active) attacks. The models are susceptible to adversarial manipulations of their training set, parameters, and inputs. The attacker can degrade the model’s predictive power, or change its behavior according to the adversary’s objective, by poisoning the training set [8, 11, 18, 27], or its parameters [2]. It is also possible to adversarially and stealthily manipulate a normal data point to confuse the model to make a wrong prediction [22]. The models can also leak significant amount of information about their training data, parameters, and inputs. Having access to the model predictions or parameters, an adversary can infer sensitive information about the model’s training set [19]. The model predictions can also be exploited to reconstruct the model parameters [23], or infer information about its input [9]. There is a large body of research on various types of these attacks and countermeasures against them, under black-box and white-box access settings, and centralized and distributed learning settings.

In this paper, we focus on active adversarial attacks against machine learning algorithms. We specifically focus on a class of attacks known as backdoor attacks, where the adversary manipulates training data and/or the training algorithm and parameters of the model in order to embed an adversarial (classification) rule into the model [8, 11]. The model behaves normally on all inputs, except for the inputs that contain the adversary’s embedded pattern, called the backdoor trigger. Several types of backdoor triggers have been explored in previous studies. These include input-instance triggers where the backdoor instances correspond to specific inputs in the input space, or pixel-pattern triggers that contain a specific pixel pattern, e.g., the images that contain a stamp, and also semantic triggers where the backdoor instances contain a specific high-level feature, e.g., objects with a particular shape or color. Figure 2 shows an example of an image with a backdoor trigger. Given the range of possible applications deep neural networks have, backdoor attacks have the ability to cause serious damage, from bypassing facial recognition authentication systems using specially crafted accessories [8], to causing driverless vehicles to misclassify stop signs using Post-it notes [11].

There are a number of detection algorithms which are designed to mitigate the risk of machine learning backdoors [7, 8, 15, 16, 24]. The detection algorithms focus on identifying which inputs contain backdoor, and which parts of the model (its activation functions specifically) are responsible for triggering the adversarial behavior of the model. For a given adversary model, the detection algorithms try to identify the signatures of the backdoors in the hidden layers of the model, in order to distinguish backdoor-enabled inputs from clean benign inputs. Note that the backdoor is an exception in the main machine learning model, thus to learn it along with the main task, the learning algorithm tries to minimize the conflict between the two. This is what the detection algorithms rely on. These algorithms compute various types of statistics on the latent representations of inputs that can help them to separate adversarial and benign data, relying on the dissimilarity of their latent representation distributions.

The common implicit assumption of all these defense techniques is that the attack is static and the adversary is unaware of the detection algorithm. Ignoring strategic attack algorithms is the main limitation of many defense techniques in adversarial machine learning. In the case of adversarial examples, it has been extensively shown that a large number of defense mechanisms can be bypassed, for the same weakness in their threat model [1, 5, 6]. In this paper, we design an **adversarial backdoor embedding** algorithm for deep learning, that maximizes the latent indistinguishability of backdoor-enabled adversarial inputs and benign inputs. We show that an attack strategy can be tailored to any particular detection algorithm and the statistics that they use for identifying backdoors. But, we go beyond bypassing specific algorithms. To be effective



Figure 1: Example of a clean image



Figure 2: Example of an image with injected backdoor trigger

against all detection algorithms, we maximize the latent indistinguishability of input data, using adversarial regularization.

We rely on data poisoning and adversarial regularization in our backdoor embedding attack. We construct a discriminator network which optimizes for identifying any difference between the benign and adversarial (backdoor-enabled) data in the hidden layers of the model. The objective function for the classification model is regularized to maximize the loss of the discriminator. Thus, the final model is not only accurate on classifying benign data points according to their label, and adversarial data points according to their adversarial label, but also has indistinguishable latent representation for data points in these two sets. This enables our algorithm to bypass the detection algorithms.

Our adversarial embedding attack successfully evades several state-of-the-art defenses. For a VGG model trained on the CIFAR-10 dataset, the dataset filtering defense using spectral signatures [24] is able to bring down the backdoor attack success rate of a compromised model to 1.5%, assuming a static attack strategy. But, a model compromised with our adversarial backdoor embedding algorithm is able to retain an attack success rate of 97.3%, against the detection algorithm. The dataset filtering defense using activation clustering [7] is similarly able to bring down the attack success rate of a compromised model to 1.9%, but our adversarial embedding algorithm retains a 96.2% attack success rate, against the detection algorithm. Feature pruning [25] is able to effectively select neurons to prune for a model, and is able to completely remove the backdoor behavior with almost no loss in model accuracy, assuming the baseline static attack. However, for a model with adversarial embedding, the full removal of the backdoor behavior simultaneously degrades the model accuracy to 20% (where 10% is the random guess). Thus, all existing detection algorithms fail against the adversarial backdoor embedding algorithm.

2 BACKDOOR DEFENSE: DETECTION ALGORITHMS

We denote the input space of the model as X , where each input instance x comes with its corresponding class label y . Backdoor attacks are defined by a backdoor trigger, which is a property B on each input in the input space, such that $\forall x \in X, B(x) \implies y = y_t$, where y_t is a target label of the attacker’s choice. We will term the set of input instances for which B hold backdoor instances for brevity.

Consider two input-label pairs, i) a clean input instance x_c and its corresponding label y_c , as well as ii) a backdoor input instance x_b that has a true class label y_b^{true} , but is wrongly classified as the target label $y_b = y_c$ due to the presence of the backdoor. Even though both input instances have the same target label, x_c contains high-level features corresponding to its true class y_c , while x_b contains high-level features corresponding to both its true class y_b^{true} and the backdoor trigger.

A hidden layer in a deep learning network can be treated as the model’s latent representation of the input instance, with the neurons in the layer representing different high-level features of the input instance. Given the high-level features present in x_c and x_b differ, one expects the respective latent representations of these input instances to also differ considerably. Several studies have successfully leveraged this difference in latent representations to detect, or to mitigate the backdoor behavior. While any hidden layer can be treated as the latent representation of the inputs, the defenses are typically applied to the penultimate layer, since it represents the highest-level features extracted by the model.

The proposed defenses we analyze fall into two main categories. The first category of defenses, given a poisoned model, uses its latent representations of clean and poisoned instances to determine neurons to prune, in order to remove the backdoor behavior from the network. The second category of defenses uses the latent representations to filter the training dataset, in order to remove most, if not all, of the maliciously injected poisoned samples. The model can then be retrained on the remaining samples to obtain a functional classifier without the backdoor behavior.

2.1 Feature Pruning

Wang et al., 2019 [25] formulate a detection technique that requires a known subset of clean inputs, detects possible backdoors, and removes them. They design a reverse-engineering process based on an optimization function that finds the minimum perturbation required to cause the misclassification of all inputs to a particular target class. This process is applied to every class in the task, yielding a candidate backdoor trigger for each class. Then, based on the intuition that a backdoor trigger is a small perturbation on the input instances, outlier detection based on the median absolute deviation is performed to detect abnormally small perturbations, which are highly likely to be the injected backdoor triggers.

Wang et al. then propose a pruning algorithm that utilizes the reverse-engineered backdoor trigger to remove the backdoor behavior from the model. It does so by recording the mean activation of each neuron n in the hidden layer over clean inputs, $\overline{z_c^n}$, and over inputs with the backdoor trigger, $\overline{z_b^n}$. Then, neurons are pruned in order of decreasing absolute difference in the means

$$\arg \max_{n \in N} |\overline{z_c^n} - \overline{z_b^n}| \quad (1)$$

The pruning is terminated when the backdoor behavior is fully removed from the model. This defense assumes that the backdoor behavior in the model is implemented by a large change in activation for the neurons that represent the backdoor features.

2.2 Dataset Filtering by Spectral Signatures

Tran, Li, and Madry, 2018 [24] propose a technique based on robust statistics to identify and remove poisoned data samples from a potentially compromised training dataset. First, a network is trained using the poisoned training dataset. For each particular output class label, all the input instances for that label are fed through the network, and their latent representations are recorded. Singular value decomposition is then performed on the covariance matrix of the latent representations, and this is used to compute an outlier score for each input. The inputs with the top scores are flagged as poisoned inputs, and removed from the training dataset. Tran et al. show that this defense succeeds when the means of the latent representations of clean inputs are sufficiently different from the means of the latent representations of backdoor inputs.

2.3 Dataset Filtering by Activation Clustering

Chen et al., 2018 [7] devise a defense that relies on clustering the latent representations of the inputs. For all input instances the model classifies as a particular class label, the latent representations of the inputs are recorded. Dimensionality reduction is performed using independent component analysis to reduce the recorded latent representations to 10 to 15 features, and k-means clustering is then performed to separate the transformed data into 2 clusters. This clustering step assumes that when projected onto the principal components, the latent representations of the backdoor inputs and clean inputs form separate clusters due to the model extracting different features from them.

Since k-means clustering produces 2 clusters regardless of whether poisoned samples are present, Chen et al. recommend a process called exclusionary reclassification to determine which of the clusters, if any, are poisoned. Consider the 2 clusters obtained for inputs the model classifies as $y_{cluster}$. A new model is trained using all training samples excluding one of the clusters. Then, the newly trained model is used to classify the input instances in the cluster. Let c_i be the number of input instances in the excluded cluster that the model classifies as label i . The ExRe score is then defined as l/p , where $l = c_{y_{cluster}}$, and $p = \max_i c_i$, $i \in L$, $i \neq y_{cluster}$. Chen et al. suggest that an ExRe score below 1 will indicate poisoning.

3 BYPASSING DEFENSES: ADVERSARIAL BACKDOOR EMBEDDING

The defenses above perform well since a significant difference in distribution of latent representations in backdoor instances and clean instances tends to emerge when a poisoned model is trained naively by the attacker. However, the defenses above fail to consider that a sophisticated attacker is able to make the model robust to them by **minimizing the difference in latent representations**. To do so, we introduce a secondary loss function to the training objective function

$$\mathcal{L}(f_{\theta}(x), y) + \mathcal{L}_{rep}(z_{\theta}(x)) \quad (2)$$

where x is the input instance, y is the target label, θ is the parameters of the network, $f_{\theta}(x)$ is the class prediction of the network for input x , and $z_{\theta}(x)$ is the latent representation of x , extracted by the network. $\mathcal{L}_{rep}(z_{\theta}(x))$ represents an additional penalty term that penalizes the model when the distributions of the network activations

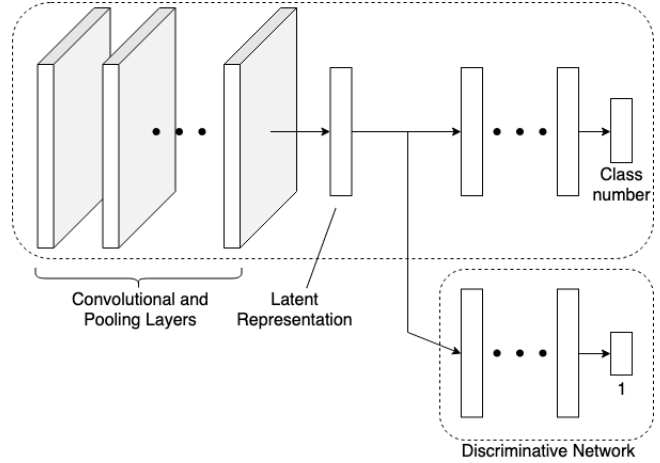


Figure 3: The architecture of our adversarial embedding attack. A discriminator is included that takes the latent representation from the model as input and decides if it is from a backdoor input or a clean input

differ greatly between clean and backdoor inputs. This additional penalty can be tailored to a specific defense that the attacker anticipates, or can be a general penalty that mitigates various defenses, as we will demonstrate. Through the double objective function, the attacker aims to achieve high classification accuracy of the model, while setting certain constraints on the latent representations of the inputs in order to bypass potential defenses.

3.1 Targeted Adversarial Embedding

We will explore an example of an attacker using the double objective function above to mitigate a specific defense. Consider the pruning defense by Wang et al. [25], which selects neurons to prune based on the absolute difference in mean neuron activations between clean and backdoor input instances, as presented in Equation 1.

In order to prevent the backdoor neurons from being selected for pruning, the attacker has to minimize $|\bar{z}_c^n - \bar{z}_b^n|$ for each neuron in the backdoor neuron set N_b . We notice that for any neuron n ,

$$|k\bar{z}_c^n - k\bar{z}_b^n| = k|\bar{z}_c^n - \bar{z}_b^n| \leq |\bar{z}_c^n - \bar{z}_b^n| \quad (3)$$

for any $0 < k < 1$. Thus, by scaling the average activation of neuron n with a sufficiently small k , we can make the defense prioritise other neurons for pruning. We thus construct our double objective function to scale the activations in the latent feature representation

$$\mathcal{L}(f_{\theta'}(x), y) + \lambda \mathcal{L}_{rep}(z_{\theta'}(x), z_{target}(x)) \quad (4)$$

where

$$z_{target}^n(x) = \begin{cases} k \cdot z_{\theta}^n(x), & \text{if } n \in N_b \\ z_{\theta}^n(x), & \text{otherwise} \end{cases}$$

λ is the regularization constant, θ is the parameters of the naively poisoned model, and θ' is the parameters of the new model. In order to obtain the set of backdoor neurons N_b , the pruning defense is first run on the naively poisoned model, and the set of neurons pruned by the algorithm (assuming the defense succeeds) will then contain mostly backdoor neurons. The additional loss function aims

to preserve the pathways of the signals in the model, but scale the amplitudes of the signals passing through any neuron in N_b by k . We use the mean square error as our loss function \mathcal{L}_{rep} .

3.2 Adversarial Embedding

While the objective function proposed above provides a convenient way for the attacker to evade one defense, it may not transfer well to other defenses. We denote the distribution of the latent representations of clean inputs as p_c , and the distribution of the latent representations of backdoor inputs as p_b . Defenses that work on the latent representations of the model, regardless of detection technique, assume the model has learned differences between the distributions p_c and p_b . These differences then inform the defense on what inputs are backdoor inputs, or what neurons correspond to backdoor features. Thus, a general form of adversarial embedding will be **one that minimizes this difference such that $p_c \approx p_b$, to prevent any significant difference from being picked up by the defenses.**

We utilise an adversarial network regularization setting (Figure 3), where we treat the initial layers up to the latent representation as a network H that outputs a latent representation given an input. Thus, we have $z_\theta(x) = H(x)$. The layers after the latent representation layer form the classification network C that maps from a latent representation to a class probability distribution. The model, then, is the composition C and H , i.e. $f_\theta(x) = C(H(x))$. We also construct a discriminative network D , that maps each latent representation $H(x)$ to a binary classification representing whether the latent representation belongs to a clean or backdoor input.

We then introduce the cost functions for D into our original objective function, obtaining

$$\mathcal{L}(f_\theta(x), y) - \lambda \mathcal{L}_D(D(H(x)), B(x)) \quad (5)$$

and an objective function for the discriminative network

$$\mathcal{L}_D(D(H(x)), B(x)) \quad (6)$$

where

$$B(x) = \begin{cases} 1, & \text{if } x \in X_b \\ 0, & \text{otherwise} \end{cases}$$

Thus, the objective of our network is to generate accurate class predictions, and at the same time extract latent representations that the discriminator is unable to classify well as clean or poisoned. We use the cross entropy loss for \mathcal{L}_D . As our training converges, we expect the distributions of latent representations for clean inputs p_c and backdoor inputs p_b to converge, such that $p_c \approx p_b$, thus minimizing any dissimilarities that the defenses rely on to detect backdoor behavior.

4 EVALUATION

4.1 Setup

We perform the above defenses on both a naively poisoned model, as well as a model trained with adversarial embedding, in order to compare the effectiveness of the defenses when facing a sophisticated attacker.

4.1.1 Datasets. We perform our evaluation on 2 image classification datasets, to show that our attack is transferrable across different applications. We use the CIFAR-10 [14] dataset which consists of 60,000 32×32 color images, equally distributed amongst 10 mutually exclusive classes. Of these images, 50,000 are used for training, and 10,000 are used for testing. We also perform our experiments on the GTSRB [21] dataset of German traffic signs. It consists of over 51,839 color images, whose dimensions range from 15×15 to 250×250 pixels (not necessarily square). The images are unevenly distributed amongst 43 mutually exclusive classes. Of these 51,839 images, 39,209 are used for training, and 12,630 are used for testing. Due to the varying sizes of the images, the images are resized to 32×32 before being passed to the model for classification.

4.1.2 Models. We perform our experiments on 2 state-of-the-art deep convolutional neural networks. Since we resize the GTSRB images to the same dimensions as the CIFAR-10 images, we are able to use the same model architecture for both datasets. The model architectures we use are the DenseNet-BC[13] model architecture with $L = 100$, $k = 12$, and the Configuration 'E' VGG [20] architecture with 19 weight layers.

4.1.3 Backdoors. We inject a backdoor trigger of a white 4×4 square at the bottom right corner in 5% of training samples, and set their labels to our arbitrarily chosen target label $y_t = 2$. We then train a model with this poisoned data, obtaining a classifier that contains the backdoor. This poisoned model forms our baseline for comparing the various defence techniques outlined above. We train

Model	Dataset	Tuning LR	Epochs	k	λ
DenseNet	GTSRB	10^{-1}	30	10^{-5}	1
VGG	CIFAR-10	10^{-1}	30	10^{-6}	1

Table 1: Parameters used in the targeted adversarial embedding attack

Model	Dataset	Epochs	Tuning LR	Discrim. LR	λ
DenseNet	CIFAR-10	30	10^{-4}	10^{-3}	50
DenseNet	GTSRB	30	10^{-4}	10^{-3}	30
VGG	CIFAR-10	1000	10^{-3}	10^{-3}	10
VGG	GTSRB	30	10^{-4}	10^{-3}	20

Table 2: Parameters used in the adversarial embedding attack

Layer	Channels	Activation
FC	256	Leaky ReLU, Batchnorm
FC	128	Leaky ReLU, Batchnorm
FC	1	Softmax

Table 3: Discriminator architecture used in adversarial embedding attack. FC stands for a fully-connected layer

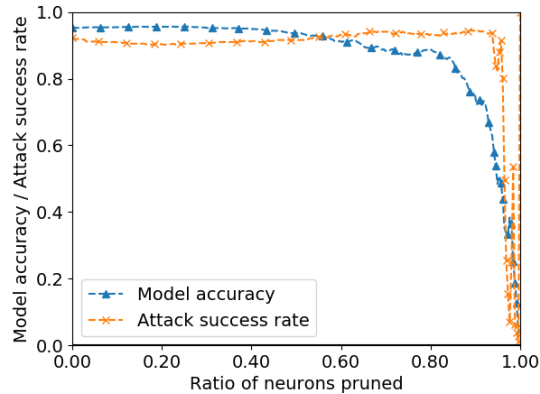


Figure 4: Attack success rate and model accuracy versus the ratio of neurons pruned when pruning [25] is performed on the baseline model (VGG, GTSRB). Pruning fails to remove the attack success rate without a significant loss in model accuracy

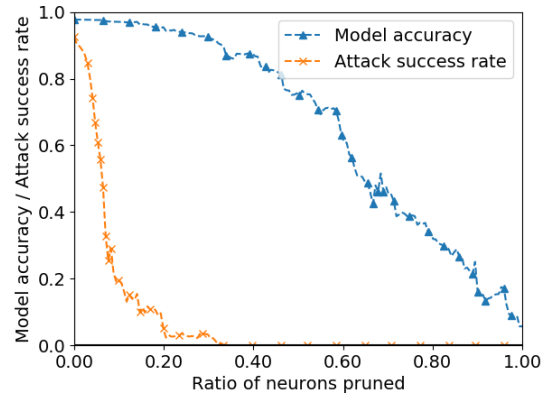
the models for 100 epochs with an initial learning rate of 0.1, which is divided by 10 at the 50th and the 75th epoch.

4.2 Results of Targeted Adversarial Embedding

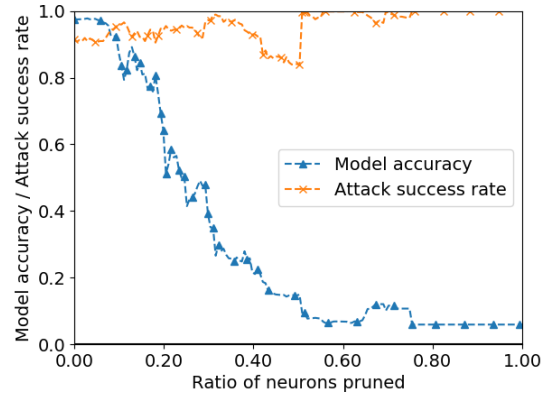
We first perform our targeted adversarial embedding on the baseline network, to evade the feature pruning defense. We assume the reverse-engineering process in the defense perfectly reconstructs the backdoor trigger, and thus we use the actual trigger described above. In order to obtain the set of backdoor neurons, the pruning defense is first performed on the baseline model, until the model accuracy falls by 8%. The pruned neurons are treated as the backdoor neurons, assuming the defense succeeds in removing the backdoor behavior. The activations of the obtained backdoor neurons are then scaled by k . To evaluate the pruning defense, we measure the model accuracy as well as the attack success rate versus the ratio of neurons in the hidden layer that are pruned. The attack success rate is simply the percentage of backdoor inputs in the test set the model classifies as the backdoor target label. For the defense to be considered successful, the attack success rate should be brought close to 0 without a substantial loss in model accuracy. The parameters used in the targeted adversarial embedding attack are listed in Table 1.

The pruning defense is not successful on the (DenseNet, CIFAR-10) run, as well as the (VGG, GTSRB) run. Figure 4 shows how the model accuracy on the (VGG, GTSRB) setting. Pruning on these settings leads to a fall in model accuracy without a corresponding fall in attack success rate in the earlier stages of pruning, and the model accuracy drops to below 40% before the backdoor behavior is removed. We thus exclude these settings from our evaluation for feature pruning.

Figure 5a shows the model accuracy and attack success rate as pruning is performed for the (DenseNet, GTSRB) setting. The attack is successful in removing the backdoor behavior with a minimal loss in model accuracy. The backdoor behavior is completely removed in



(a) Baseline model. Pruning successfully brings the attack success rate down to 0% with a small trade-off in model accuracy



(b) Model with targeted adversarial embedding. Pruning is unable to bring down the attack success rate

Figure 5: Attack success rate and model accuracy versus the ratio of neurons pruned when pruning [25] is performed (DenseNet, GTSRB)

exchange for about an 8% reduction in model accuracy, thus minimal fine-tuning is required to restore the model accuracy. However, the pruning defense is unable to remove the backdoor from the models with targeted adversarial embedding. Figure 5b shows the effect of pruning on our defense-aware model. The pruning algorithm selects clean neurons to prune over the backdoor neurons, thus we see the model accuracy fall dramatically when pruning is performed on the network. Furthermore, as the clean neurons are removed, the relative magnitude of the backdoor signals increases, and we see the attack success rate increasing.

4.3 Results of Adversarial Embedding

We then perform our adversarial embedding attack on the baseline model. The parameters of our attack are recorded in Table 2. 30 epochs is sufficient for the attack to mitigate the dataset filtering defenses based on activation clustering and spectral signatures,

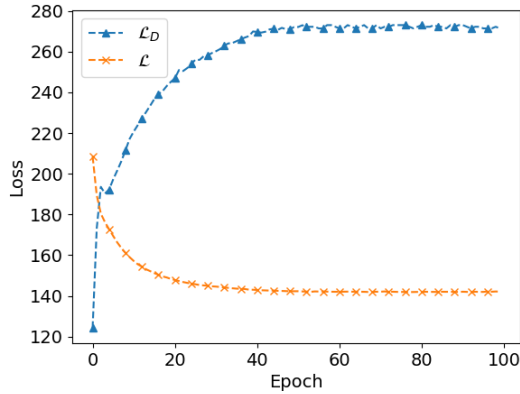


Figure 6: The discriminator loss \mathcal{L}_D (Equation 6) and the loss \mathcal{L} of the poisoned model (Equation 5) versus the epoch when adversarial training is performed. The losses converge to a constant value as the number of epochs increases

but 1000 epochs was needed to evade the pruning defense. We use a fully connected discriminator with a leaky ReLU activation and negative slope of 0.2, as well as batch norm in each of the layers. The architecture of the discriminator is described in Table 3. Noise sampled from a Gaussian distribution $\mathcal{N}(0, \sigma^2)$ is added to the discriminator inputs. σ begins at 0.1, and is decreased by a factor of 10 each epoch. We use a weight decay of 0.9. Figure 6 shows how the losses of the discriminator and the poisoned model converge to their final values as the adversarial embedding attack is carried out.

Figure 7 shows effect of pruning on the model accuracy and the attack success rate of the VGG model adversarially trained on the CIFAR-10 dataset. While the model is noticeably less robust to the pruning defense than the one trained with targeted adversarial embedding, the model still preserves a significant percentage of the attack success rate as the model accuracy falls. The defense is no longer able to completely remove the backdoor behavior from the model without requiring significant retraining to restore the original model accuracy.

We next evaluate the dataset filtering defense based on spectral signatures [24]. Table 4 shows the number of poisoned training samples present in the training set before and after the defense is carried out. We use an ϵ equal to the percentage of poisoned samples in the backdoor target label, so a total of $(1.5 \cdot \epsilon)\%$ of samples with the given label are removed. The defense works well on the baseline model, in most cases removing all but less than 2% of poisoned samples within the training dataset. However, our adversarial embedding of the backdoor successfully mitigates the detection algorithm, leaving more than half of the poisoned samples in the training dataset. We retrain models on the filtered training datasets, and record the attack success rate on the new models in Table 4. The defense is successful on the baseline models, and the attack success rate on the retrained model is low (0% to 1.5%), but the retrained models from the model with adversarial embedding

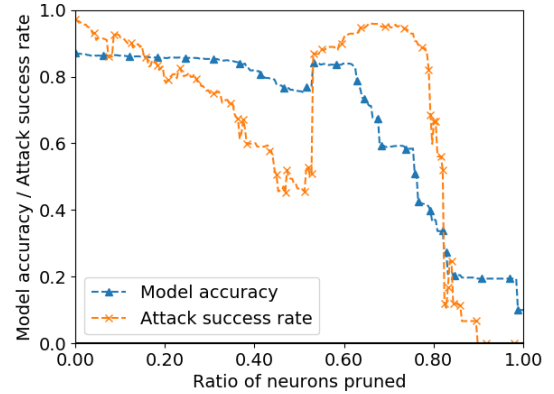


Figure 7: Attack success rate and model accuracy versus the ratio of neurons pruned when pruning [25] is performed on the model with adversarial embedding (VGG, CIFAR-10). Pruning completely removes the backdoor behavior at the cost of bringing the model accuracy down to 20%

retains the backdoor behavior, and we see an attack success rate of above 90%.

To understand why our attack evades the defense, we analyze the correlations of the latent representations with the top eigenvector produced from singular value decomposition. This is the mechanism used by the defense to remove poisoned samples from the dataset. Figure 8a shows the correlations for the baseline model with the (VGG, CIFAR-10) setting. The distribution of correlations of the representations of the poisoned inputs (in red) are noticeably different from that of the clean inputs (in blue), with the representations of the poisoned inputs having much higher correlations. A large fraction of poisoned inputs can thus be removed by removing the inputs whose latent representations have the highest correlations. On the other hand, the **latent representations yield a similar distribution of correlations for the model with adversarial embedding**, as shown in Figure 8b. The poisoned inputs in the dataset no longer exhibit a larger correlation, and removing inputs with the highest correlations is not sufficient to remove the majority of the poisoned inputs from the training dataset, since poisoned samples and clean samples are both removed at the same rate.

We now evaluate the dataset filtering defense based on activation clustering, proposed by Chen et al. [7]. The defense consists of two main steps – clustering, and performing additional detection steps on the resultant clusters. We notice that the detection methods assume a clean split between the poisoned samples and the clean samples. For example, the exclusionary reclassification step assumes that the newly trained model does not contain the backdoor behavior, and classifies the poisoned samples as their true class. Thus, we evaluate the quality of the clustering step using the adjusted Rand index to evaluate the quality of the clustering. Then, the perfect separation of poisoned and clean samples will give a score of 1, while random separation of the samples will give a score of 0. We also retrain the model on the filtered dataset assuming

Model	Dataset	ϵ	# Pois	# Pois Left (Baseline)	# Pois Left (Adversarial Embedding)	Attack Success (Baseline)	Attack Success (Adversarial Embedding)
DenseNet	C10	31	2241	37 (1.7%)	1406 (63.0%)	1.1%	97.3%
DenseNet	GTSRB	46	1844	27 (1.5%)	1263 (68.5%)	0.0%	89.9%
VGG	C10	31	2241	54 (2.4%)	1050 (46.9%)	1.5%	97.3%
VGG	GTSRB	46	1844	11 (0.6%)	1004 (54.4%)	0.3%	90.3%

Table 4: Number of poisoned samples left in the dataset, as well as the attack success rate on the retrained models for the dataset filtering defense based on spectral signatures [24]. The defense removes most poisoned samples from the baseline model, but fails to do so for the model with adversarial embedding

Model	Dataset	Rand Index (Baseline)	Rand Index (Adversarial Embedding)	Attack Success (Baseline)	Attack Success (Adversarial Embedding)
DenseNet	CIFAR-10	0.979	0.182	1.7%	76.4%
DenseNet	GTSRB	0.997	0.271	0.0%	91.4%
VGG	CIFAR-10	0.998	6.31×10^{-4}	1.9%	96.2%
VGG	GTSRB	0.997	0.642	1.1%	74.3%

Table 5: Adjusted Rand indexes of the clusters formed from k-means clustering with $k = 2$ in the defense based on activation clustering [7], as well as the attack success rate on the models retrained on the filtered dataset. A Rand index close to 1 represents a good separation of clean and poisoned inputs in the clustering step, while a Rand index close to 0 represents poisoned inputs are present in both sets. Adversarial embedding is able to significantly reduce the quality of clustering, and thus the retrained model still contains the backdoor behavior

the best resultant cluster is selected for removal, i.e. the resultant cluster with the highest fraction of poisoned samples is removed. In the clustering step of the defense, we perform independent component analysis to reduce the latent representations to 10 independent components, before running k-means clustering with $k = 2$.

Table 5 shows the adjusted Rand scores of the clusters formed, as well as the attack success rate on the retrained model for both the baseline, and the model with adversarial embedding. The defense works well on the baseline model, attaining almost perfect clustering of the clean and poisoned samples (adjusted Rand index > 0.95), and the attack success rate on the retrained models is very low (0% to 1.9%). However, our attack successfully mitigates this defense technique, yielding a lower resultant adjusted Rand index after the clustering step. This signifies that a significant number of poisoned samples is present in both resultant clusters. Thus, the model retrained on the resultant filtered dataset still contains the backdoor behavior, and exhibits a high attack success rate of above 75%.

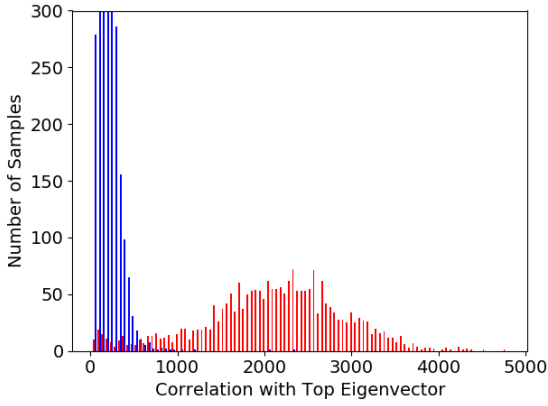
To understand why our attack evades the defense, we analyze the latent representations of the VGG model trained on the CIFAR-10 dataset. Figure 9a shows the latent representations of all inputs by the baseline model, projected onto the top two independent components. The poisoned inputs (in red) form a noticeably disjoint cluster from the clean inputs (in blue). Thus, k-means clustering can separate the poisoned inputs from the clean inputs well, and most of the poisoned samples can be removed from the training dataset by excluding the right cluster. Figure 9b shows the latent representations for the model with adversarial embedding, similarly projected onto the top two independent components. **The adversarial training causes the poisoned and clean latent representations to**

overlap significantly due to a convergence in their distributions, so k-means clustering is unable to separate the poison inputs from the clean inputs well. Thus, removing either of the resultant k-means clusters still leaves a significant number of poisoned sample in the training dataset, and the retrained model will still contain the backdoor.

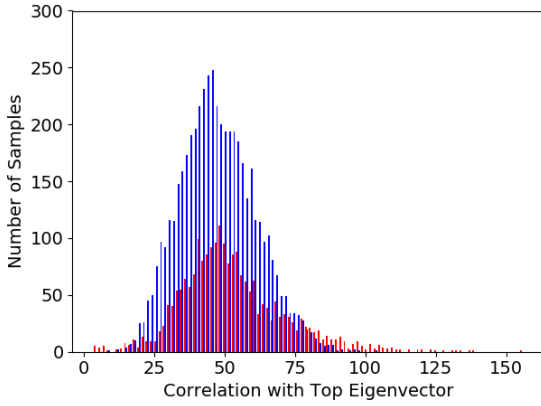
5 RELATED WORK

Backdoors in deep learning networks is a topic of growing interest. Many studies explore backdoor injection through data poisoning, where the attacker injects maliciously crafted input and label samples into the training dataset [8, 11, 18]. These poisoned inputs are typically images with the backdoor trigger superimposed, and the target label altered. It has been shown that a small number of poisoned data points (50 samples) is needed to introduce a backdoor with a high attack success rate ($>90\%$) [8]. It has been shown that the introduced backdoors persist after the model is repurposed [11]. Thus, malicious behavior injected in models up the supply chain can propagate to downstream models, even if the retraining is done with a clean dataset. Many approaches to data poisoning lead to a visible trigger superimposed on the poisoned images, which makes malicious training data apparent to human eyes, but it has been shown to be possible to generate poison data that looks clean, and with unaltered class labels [18].

Backdoor attacks that do not rely on the attacker having access to the training data have also been devised. In the federated learning setting, the attacker has the ability to broadcast weight updates to the other parties. This ability can be exploited to broadcast weight updates that introduce backdoor behavior to the models that



(a) Baseline model. The poisoned representations have a significantly higher correlation than the clean representations, and thus can be filtered by removing samples with the top correlations

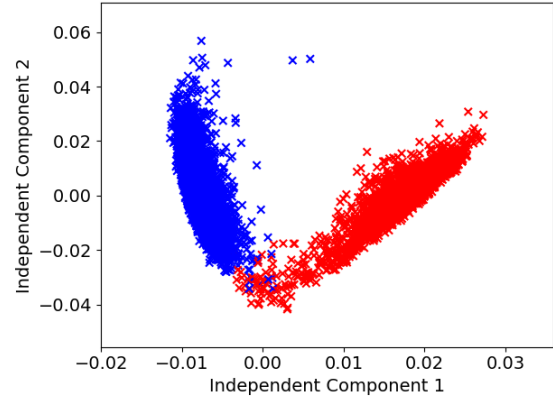


(b) Model with adversarial embedding. The poisoned and clean representations have similar distributions of correlations, and thus filtering the samples with top correlations removes an equal portion of clean and poisoned samples

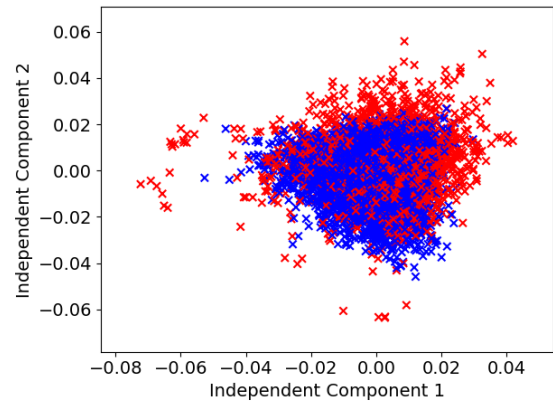
Figure 8: Correlation of latent representations of all inputs in the training dataset with the top eigenvector for the data filtering defense based on spectral signatures [24]. The representations of poisoned inputs are in red

receive the update [2]. Federated learning settings with secure aggregation are especially susceptible to this attack as the individual weight updates cannot be inspected. Furthermore, the algorithm that generates the weight updates can also take into account the anomaly detection technique used by the system, in order to bypass the defense when secure aggregation is not used. Various studies have also worked on making distributed learning settings that converge to a useful model despite the presence of Byzantine workers [4, 26, 28]. However, the guarantees that these robust algorithms provide have been shown to be insufficient [3, 17].

In response to the backdoor attacks that have been devised, there have been several papers that aim to remove backdoor behavior, besides the ones mentioned in this paper. Liu et al., 2018 [15] take



(a) Baseline model. The representations of poisoned inputs (in red) form a distinct separate cluster from the clean inputs, and thus are easily separated by k-means clustering



(b) Model with adversarial embedding. The representations of poisoned inputs (in red) have a similar distribution as those of clean inputs, thus both clusters formed by k-means clustering contain a significant number of poisoned samples

Figure 9: Latent representations of all inputs in the training dataset projected onto their top two independent components for the data filtering defense based on activation clustering [7]. The representations of poisoned inputs are in red

a similar approach of pruning neurons based on the latent representations of a known clean set of inputs, operating under the assumption that the backdoor neurons are dormant for clean inputs. Since it is possible to train a model to be robust to this pruning, Liu et al. recommend a combination of pruning and fine-tuning of the model to remove the backdoor behavior. Some backdoor mitigation techniques work on the input space of the model instead of the latent space, relying on either training a model to identify anomalous inputs, or to remove anomalous features in inputs before feeding to the model [16].

Besides backdoor attacks, there have been many studies on adversarial machine learning where the discontinuous input-output

mappings of deep learning networks are exploited to generate adversarial images that resemble image of a particular class, but the model misclassifies [10, 22]. It has also been shown to be possible to generate adversarial images by perturbing the color space of the image, thus preserving the smoothness of the image, in order to evade detection methods that rely on the abrupt pixel changes found in many adversarial image detection methods [12].

6 CONCLUSIONS

While backdoor detection using the learned latent representations greatly reduces the dimensionality and thus complexity of the defense technique, we have showed that a sophisticated attacker is easily able to hide the signals of the backdoor images in the latent representation, rendering the defense ineffective. We designed a novel adversarial embedding attack that successfully mitigates several published defenses against backdoor attacks that rely on the latent representations of the network. Furthermore, we demonstrated the effectiveness of a targeted adversarial embedding attack that bypasses a specific defense of the attacker's choice. However, while our attack hides the signals of a particular hidden layer in the network, it is conceivable that the backdoor signals are still apparent in other layers of the network, thus the defense may attempt to look at multiple layers of the network in unison in order to detect these signals. A form of adversarial embedding that takes into account all layers in the network thus remains as a topic of future research.

REFERENCES

- [1] Anish Athalye, Nicholas Carlini, and David Wagner. 2018. Obfuscated gradients give a false sense of security: Circumventing defenses to adversarial examples. *arXiv preprint arXiv:1802.00420* (2018).
- [2] Eugene Bagdasaryan, Andreas Veit, Yiqing Hua, Deborah Estrin, and Vitaly Shmatikov. 2018. How to backdoor federated learning. *arXiv preprint arXiv:1807.00459* (2018).
- [3] Moran Baruch, Gilad Baruch, and Yoav Goldberg. 2019. A Little Is Enough: Circumventing Defenses For Distributed Learning. *arXiv preprint arXiv:1902.06156* (2019).
- [4] Peva Blanchard, Rachid Guerraoui, Julien Stainer, et al. 2017. Machine learning with adversaries: Byzantine tolerant gradient descent. In *Advances in Neural Information Processing Systems*. 119–129.
- [5] Nicholas Carlini and David Wagner. 2017. Adversarial examples are not easily detected: Bypassing ten detection methods. In *Proceedings of the 10th ACM Workshop on Artificial Intelligence and Security*. ACM, 3–14.
- [6] Nicholas Carlini and David Wagner. 2017. Towards evaluating the robustness of neural networks. In *2017 IEEE Symposium on Security and Privacy (SP)*. IEEE, 39–57.
- [7] Bryant Chen, Wilka Carvalho, Nathalie Baracaldo, Heiko Ludwig, Benjamin Edwards, Taesung Lee, Ian Molloy, and Biplav Srivastava. 2018. Detecting backdoor attacks on deep neural networks by activation clustering. *arXiv preprint arXiv:1811.03728* (2018).
- [8] Xinyun Chen, Chang Liu, Bo Li, Kimberly Lu, and Dawn Song. 2017. Targeted backdoor attacks on deep learning systems using data poisoning. *arXiv preprint arXiv:1712.05526* (2017).
- [9] Matthew Fredrikson, Eric Lantz, Somesh Jha, Simon Lin, David Page, and Thomas Ristenpart. 2014. Privacy in pharmacogenetics: An end-to-end case study of personalized warfarin dosing. In *23rd {USENIX} Security Symposium ({USENIX} Security 14)*. 17–32.
- [10] Ian J Goodfellow, Jonathon Shlens, and Christian Szegedy. 2014. Explaining and harnessing adversarial examples. *arXiv preprint arXiv:1412.6572* (2014).
- [11] Tianyu Gu, Brendan Dolan-Gavitt, and Siddharth Garg. 2017. Badnets: Identifying vulnerabilities in the machine learning model supply chain. *arXiv preprint arXiv:1708.06733* (2017).
- [12] Hossein Hosseini and Radha Poovendran. 2018. Semantic adversarial examples. In *Proceedings of the IEEE Conference on Computer Vision and Pattern Recognition Workshops*. 1614–1619.
- [13] Gao Huang, Zhuang Liu, Laurens Van Der Maaten, and Kilian Q Weinberger. 2017. Densely connected convolutional networks. In *Proceedings of the IEEE conference on computer vision and pattern recognition*. 4700–4708.
- [14] Alex Krizhevsky and Geoffrey Hinton. 2009. *Learning multiple layers of features from tiny images*. Technical Report. Citeseer.
- [15] Kang Liu, Brendan Dolan-Gavitt, and Siddharth Garg. 2018. Fine-pruning: Defending against backdooring attacks on deep neural networks. In *International Symposium on Research in Attacks, Intrusions, and Defenses*. Springer, 273–294.
- [16] Yuntao Liu, Yang Xie, and Ankur Srivastava. 2017. Neural trojans. In *2017 IEEE International Conference on Computer Design (ICCD)*. IEEE, 45–48.
- [17] El Mahdi El Mhamdi, Rachid Guerraoui, and Sébastien Rouault. 2018. The hidden vulnerability of distributed learning in byzantium. *arXiv preprint arXiv:1802.07927* (2018).
- [18] Ali Shafahi, W Ronny Huang, Mahyar Najibi, Octavian Suci, Christoph Studer, Tudor Dumitras, and Tom Goldstein. 2018. Poison frogs! targeted clean-label poisoning attacks on neural networks. In *Advances in Neural Information Processing Systems*. 6103–6113.
- [19] Reza Shokri, Marco Stronati, Congzheng Song, and Vitaly Shmatikov. 2017. Membership inference attacks against machine learning models. In *2017 IEEE Symposium on Security and Privacy (SP)*. IEEE, 3–18.
- [20] Karen Simonyan and Andrew Zisserman. 2014. Very deep convolutional networks for large-scale image recognition. *arXiv preprint arXiv:1409.1556* (2014).
- [21] Johannes Stalkamp, Marc Schlipfing, Jan Salmen, and Christian Igel. 2011. The German Traffic Sign Recognition Benchmark: A multi-class classification competition. In *IEEE International Joint Conference on Neural Networks*. 1453–1460.
- [22] Christian Szegedy, Wojciech Zaremba, Ilya Sutskever, Joan Bruna, Dumitru Erhan, Ian Goodfellow, and Rob Fergus. 2013. Intriguing properties of neural networks. *arXiv preprint arXiv:1312.6199* (2013).
- [23] Florian Tramèr, Fan Zhang, Ari Juels, Michael K Reiter, and Thomas Ristenpart. 2016. Stealing machine learning models via prediction apis. In *25th {USENIX} Security Symposium ({USENIX} Security 16)*. 601–618.
- [24] Brandon Tran, Jerry Li, and Aleksander Madry. 2018. Spectral signatures in backdoor attacks. In *Advances in Neural Information Processing Systems*. 8000–8010.
- [25] Bolun Wang, Yuanshun Yao, Shawn Shan, Huiying Li, Bimal Viswanath, Haitao Zheng, and Ben Y Zhao. 2019. Neural cleanse: Identifying and mitigating backdoor attacks in neural networks.
- [26] Cong Xie, Oluwasanmi Koyejo, and Indranil Gupta. 2018. Generalized byzantine-tolerant sgd. *arXiv preprint arXiv:1802.10116* (2018).
- [27] Chaofei Yang, Qing Wu, Hai Li, and Yiran Chen. 2017. Generative poisoning attack method against neural networks. *arXiv preprint arXiv:1703.01340* (2017).
- [28] Dong Yin, Yudong Chen, Kannan Ramchandran, and Peter Bartlett. 2018. Byzantine-robust distributed learning: Towards optimal statistical rates. *arXiv preprint arXiv:1803.01498* (2018).